



Development of a New Experimental Technique for Dynamic Fracture Toughness Measurement of Rocks using Drop Weight Test

G. Khandouzi, H. Memarian and M.H. Khosravi*

School of Mining Engineering, College of Engineering, University of Tehran, Tehran, Iran

Received 20 June 2020; received in revised form 8 July 2020; accepted 9 July 2020

Keywords

Dynamic fracture toughness

Drop weight

Numerical simulation

Limestone

Abstract

The dynamic fracture characteristics of rock specimens play an important role in analyzing the fracture issues such as blasting, hydraulic fracturing, and design of supports. Several experimental methods have been developed for determining the dynamic fracture properties of the rock samples. However, many used setups have been manufactured for metal specimens, and are not suitable and efficient for rocks. In this work, a new technique is developed to measure the dynamic fracture toughness of rock samples and fracture energy by modifying the drop weight test machine. The idea of wave transmission bar from the Hopkinson pressure bar test is applied to drop weight test. The intact samples of limestone are tested using the modified machine, and the results obtained are analyzed. The results indicate that the dynamic fracture toughness and dynamic fracture energy have a direct linear relationship with the loading rate. The dynamic fracture toughness and dynamic fracture energy of limestone core specimens under the loading rates of 0.12-0.56kN/ μ S are measured between 9.6-18.51MPa \sqrt{m} and 1249.73-4646.08J/m², respectively. In order to verify the experimental results, a series of numerical simulation are conducted in the ABAQUS software. Comparison of the results show a good agreement where the difference between the numerical and experimental outputs is less than 4%. It can be concluded that the new technique on modifying the drop weight test can be applicable for measurement of the dynamic behavior of rock samples. However, more tests on different rock types are recommended for confirmation of the application of the developed technique for a wider range of rocks.

1. Introduction

Fracture mechanics has been applied for a variety of rock engineering issues such as rock cutting, explosive fracturing, seismic events, and hydro fracturing, which is based on the Griffith theory and the Irvin's modification for cracked medium under the static or dynamic conditions [1]. Understanding the behavior of the materials under static or dynamic fracturing is essential. This behavior is described by the fracture parameters such as the dynamic fracture energy and dynamic fracture toughness, indicating the resistance of materials against the propagation of the pre-existing cracks [2]. Earlier measurements of the stress intensity factor (SIF) followed the ASTM-

E399 standard method for static load. Due to the fact that most of the rocks are brittle with pre-cracking fatigue properties, the above-mentioned ASTM standard method is not so efficient [3]. Therefore, the International Society for Rock Mechanics (ISRM) recommended three methods for determination of the static fracture parameters of core-based rock specimens [4]. ISRM suggested the Short Rod (SR) and the Chevron Bending (CB) tests for fracture test in 1988 [5] and the Cracked Chevron Notched Brazilian Disc (CCNBD) in 1995 [6]. In addition to the methods suggested by ISRM for the static condition, many researchers have used different sample geometries to measure

dynamic fracture parameters; for example, Chunan and Xiaohe (1990) used cubic-shaped samples of a marble specimen [7]. Wang *et al.* (2011-2009) have determined this property using the holed-cracked flattened Brazilian discs and cracked straight-through flattened Brazilian discs [8, 9]. Nikita *et al.* (2009) have examined the static and dynamic SIF of a few different rock types [10]. Chen *et al.* (2009) used NSCB and Dai *et al.* (2010-2011) tested CCNBD to determine the dynamic fracture toughness of granites [11, 12]. Recently, some researchers have used the notched semi-circle bend specimens in order to specify the rock dynamic fracture features under different loading rates [13, 14]. Liu *et al.* (2019) have investigate the effects of two elliptical holes and four fissures on the mechanical behavior of sandstone using the acoustic emission (AE) monitoring and digital image correlation (DIC) techniques [15]. Among the experimental methods proposed by ISRM and ASTM for measurement of the dynamic fracture parameters, the Charpy impact test, the drop weight test, and the Hopkinson pressure bar are the most common experimental techniques illustrated in Figure 1, and the advantages and disadvantages of those techniques are summarized in Table 1. Alongside many published papers in the field of rock fracture toughness estimation, the Hopkinson pressure bar has been used to conduct the fracture tests in order to measure the dynamic stress intensity factor (DSIF). This test is useful for metallic materials and small piece of rock specimens [20]. The Charpy test is used to measure the K_{IC} values [21]. The ASTM standard E208 has

been introduced the drop weight machine as a standard laboratory setup, which is able to test a variety of large specimens including the edge-notched specimens under the 3-point bending (3PB) mechanism. There are some limitations for using the drop weight test. Those limitations are due to a sudden impact in the drop weight test, which leads to a jump of the specimen from its supports. It may result in a lack of recording of the reflected wave from the interface of the specimen and the tub head, therefore, the stress equilibrium during the test may not be achieved. The rate and the form of the compressive load depend on both the specimen and the features of the machine. Moreover, great care should be taken in interpreting experimental data due to the coupling effects between the machine vibration and the wave propagation. In this situation, the loading rate cannot be well controlled; thus, multi-axial loadings are unreliable [22]. Due to the limitations of the above-mentioned common experimental setups for measurement of dynamic fracture toughness of rock samples, it has been decided to develop a new experimental technique for measurement of the rock dynamic fracture based on the drop weight test. In this paper, the rock dynamic fracture is studied experimentally. In the first step, the modified setup is introduced, and then the way of determination dynamic fracture toughness is described. Finally, the test results of core specimens with the straight notch crack in 3PB for the limestone are presented and the comparison with the numerical results is discussed.

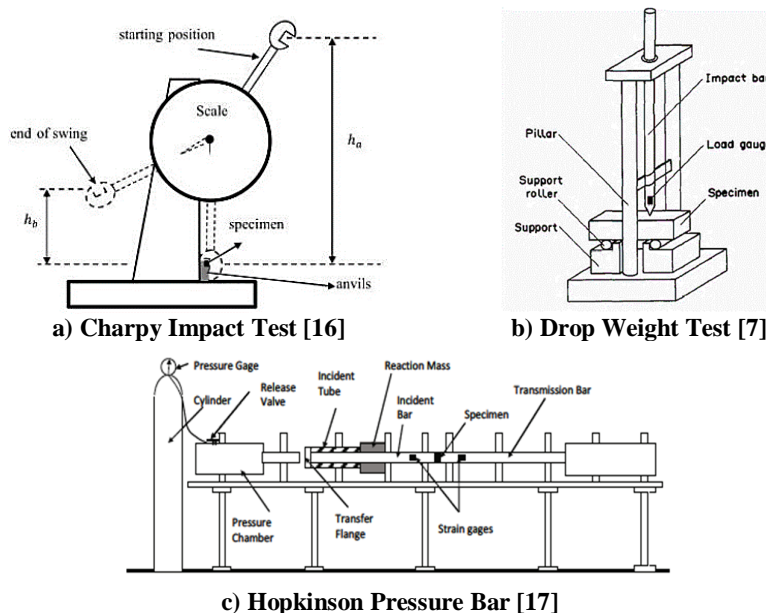


Figure 1. Most common experimental dynamic fracture tests.

Table 1. Advantages and disadvantages of most common experimental dynamic fracture tests [18, 19].

Name	Advantages	Disadvantages
Charpy Impact Test	- Simple setup	-Specimen jumped off the supports -Extreme fluctuations in the recorded force -A lack of understanding of the inertia force due to stress wave propagation in Charpy specimen
Drop Weight Test	- Simple setup - Using a large specimen for testing	- Specimen jumped off the supports - Not satisfaction of the stress equilibrium - Not justifying inertia force
Hopkinson Pressure Bar	- Inertia can be ignored - Specimen reaches stress equilibrium before failure -Loading sample with constant rate before failure point	-Using a small piece of rock specimen

2. Modified drop weight test

In order to solve the above-mentioned limitations of the common tests, the idea of wave transmission bar was borrowed from the Hopkinson pressure bar test and applied to the drop weight test and a modified drop weight test setup was developed. The modified drop weight test apparatus is illustrated in Figure 2.

By this technique, in the modified drop weight test setup, the specimen won't jump of when the weight is dropped. Consequently, it will easily achieve stress equilibrium, and the reflected wave from interface of specimen and tub head can be recorded. Furthermore, the rate and form of the compressive loading is not dependent on the features of the specimen and machine. As well, the average energy and the loading rate can be well-controlled by means of the height and weight of

falling weight on the transmission bar. Another advantage of the modified setup system is that the larger rock specimens could be tested in a variety of forms including disc-shaped, cylindrical, and cubic.

In order to measure the dynamic load applying to the specimen, a strain gauge was mounted at the end of the transmission bar (Figure 2). The position of the strain gauge on the transmission bar is extremely important as we have to deal with two problems. First, at high rates of loading, the striker material's inertia forces are not entirely negligible in comparison to the contact forces between the specimen and the striker. Another problem is that the measured strain is dependent on the distribution of load over the specimen/striker contact region [23].

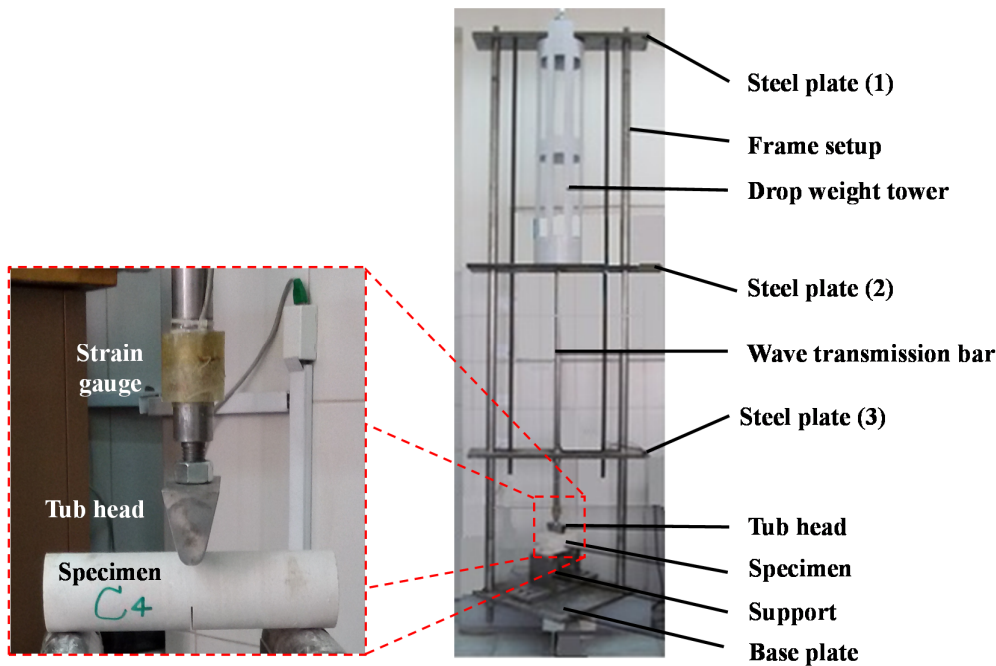


Figure 2. A modified drop weight test setup for measurement of dynamic fracture toughness of rock samples.

When the strain gauges are moved closer to the contact surface, the inertia effects become smaller due to the reduced intervening mass. By contrast, the contact force distribution effects can be reduced by moving the strain gauge away from the contact surface. Therefore, strain gauge should be mounted on the correct position of the transmission bar to reduce errors due to inertia forces as well as decrease force distribution. Also when wave propagates along the transmission bar, the wave continually changes its amplitude and shape due to damping losses and wave dispersion [24]. As a result, it is better to mount the strain gauge near the tub head to solve all the problems mentioned above. Thus by analyzing a considerable number of the test results, it was concluded that in the modified drop weight test apparatus, the strain gauge should be mounted on the transmission bar in a 10 cm distance from the tub head (Figure 2).

2.1. Strain gauge and recording system

Since dynamic tests are rather expensive and time-consuming, the sensors and data logger must be able to record data at an appropriate speed [24]. In this type of test, strain gauges are often preferred. Dynamic strain measurement can be carried out by means of three different types of strain gauges, Foil Strain Gauge (FSG), Semiconductor Strain Gauge (SSG) and Polyvinylidene Fluoride strain gauge (PVDF). FSG is the most common sensor in the

experiment’s analysis [24]. In addition, to save data detected by strain gauge, a data acquisition system shown in Figure 3 is used in this work. This consists of a digital oscilloscope DS 1064 B that has four-channel with 2Gsa/s sampling precision, and an electrical circuit includes an amplifier and Wheatstone bridge and battery (6 volt).

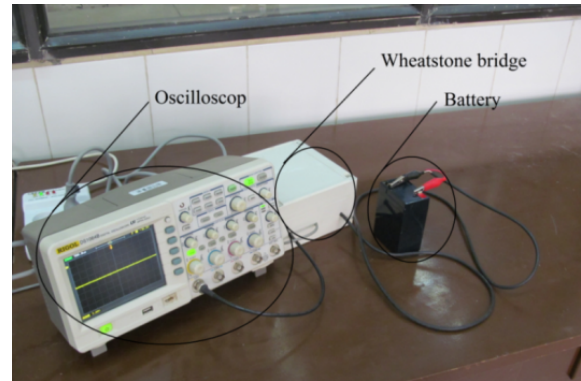


Figure 3. Data acquisition system used in this work.

Dynamic wave, detected by oscilloscope, is recorded in the .rcd format, which can be processed and converted to bit map (.bmp) image files by the Ultra-scope software. For digitizing the .bmp format of images in Ultra-scope, an algorithm was written in the Matlab software, as illustrated in the flowchart of Figure 4.

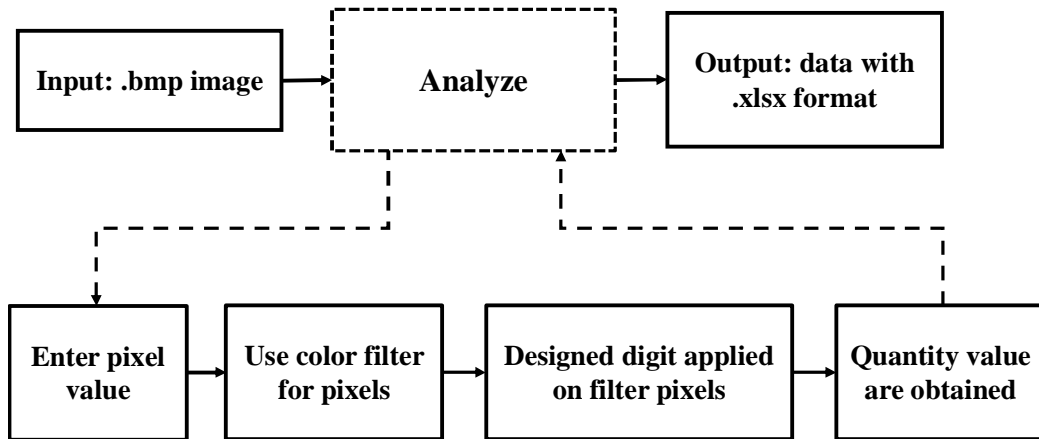


Figure 4. A flowchart of the algorithm written in MATLAB.

2.2. Calibration of data acquisition system

Since the oscilloscope detects voltage, calibration is necessary to find out an appropriate relationship between the impact force and the reported voltage. There are basically two methods of calibration:

direct and indirect. Direct calibration has been adopted to calibrate and convert voltage of output of oscilloscope to the equivalent force. Calibration and force–voltage graph for the Modified Drop Weight machine is shown in Figure 5.

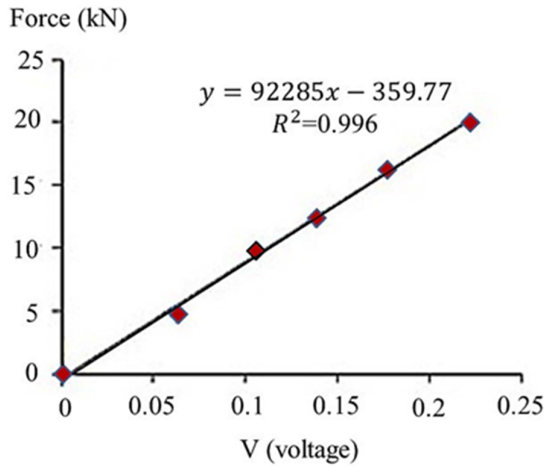


Figure 5. Calibration force-voltage relation graph.

The primary output of oscilloscope contains noise, spectroscopic (peak) data, and sharp. Almost all the detected signals are noise-contaminated, which is an unpleasant phenomenon. Hence, the noise reduction techniques are very essential to reproduce a more representative signal. In filtering a signal, if the applied filter is not appropriate, the filtered signal might be deformed and some parts of data might be deleted. Amongst different filters, the Savitzky-Golay (S-G) filter [25] was selected because this filter reduced noise and kept the structure of the original signal. For achieving a model of output, a curve-fitting tool and S-G filter was used in the Matlab software. The flowchart of the data acquisition system used for the modified drop weight test apparatus is illustrated in Figure 6.

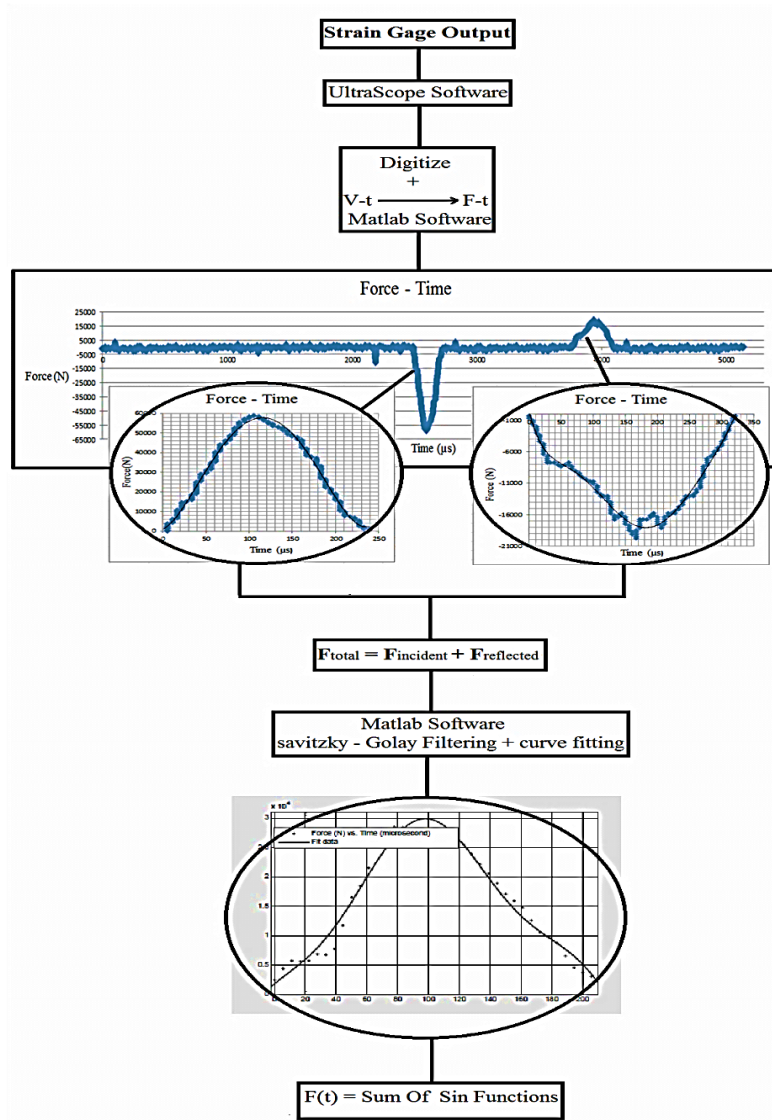


Figure 6. A flowchart of the data acquisition system.

3. Material properties and specimen preparation

The behavior of material, texture and mineralogical purity of specimen is important in the fracture tests. The specimen should have a linear elastic behavior, a uniform texture, and a high mineralogical purity. The macroscopic and microscopic studies on the limestone specimens showed that the specimens were compact with a uniform texture. They had a high mineralogical purity, and entirely consisted of fine grain bioclastic limestone with microcrystalline background texture. Therefore, the limestone was selected as an appropriate rock for this work.

For determination of the mechanical properties of the understudied limestone, the uniaxial compressive strength (UCS) tests and the Brazilian tensile strength tests were conducted. Rigid servo control press 450 tones capacity (MTS) was used for conducting the uniaxial compressive tests. During the test, strain gages were used to measure the axial and lateral deformations of the sample. The properties of the understudied limestone are listed in Table 2.

Table 2. Properties of limestone used in this work.

E (GPa)	ν	ρ ($\frac{kg}{m^3}$)	σ_c (MPa)	σ_t (MPa)
73.5	0.057	2700	26.5	9.85



a) Some specimens after testing

A total number of 9 core specimens with a diameter of $D = 54$ mm and a length of $L = 220$ mm (L) were prepared by means of a coring machine. A 1 mm-thick initial crack with a height of $a = 20$ mm was made in the middle of the length of the specimens, as illustrated in Figure 7.

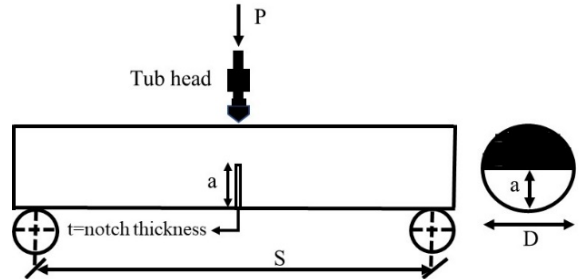
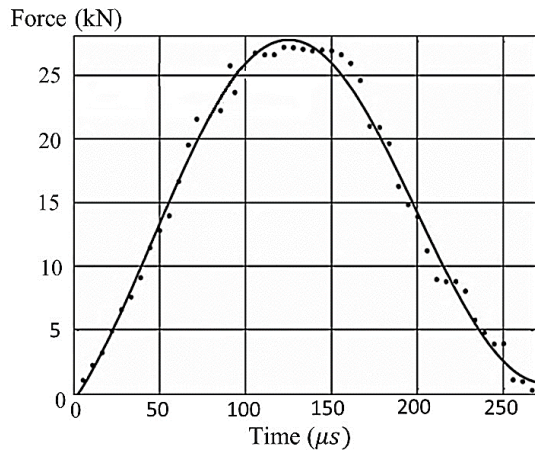


Figure 7. Geometric detail of the core specimen.

4. Experimental results

After preparation of the specimen, a weight of 3 kg was dropped from a height inside the drop weight tower. The impact of the drop weight was transferred to the specimen through the transmission bar (Figure 1). By adjusting the height of the drop weight, different dynamic loading rates were applied to the core specimens. The load was transferred to the specimen, resulting in its fracture, and was calculated from the deformation recorded by the strain gauge. The images of some specimens after failure and the load data recorded for Test 1 is shown in Figure 8.



b) The load data recorded in Test 1

Figure 8. Load data recorded and cores specimen with straight notched after test.

A curve with the best fit for the data shown in Figure 8(b) has the following sinusoidal equation.

$$F(t) = a_1 \cdot \sin(b_1 \cdot t + c_1) + a_2 \cdot \sin(b_2 \cdot t + c_2) \quad (1)$$

$$R^2 = 0.9831$$

where t is the time and $a_1, a_2, b_1, b_2, c_1, c_2$ are constant coefficients that differ for every test. The constant coefficients obtained for Test 1 are listed in Table 3.

Table 3. Values of constant coefficients for the best sinusoidal curve fit obtained for Test 1.

a_1	a_2	b_1	b_2	c_1	c_2
17780	14540	0.001	0.02043	0.6734	-0.9295

The dynamic loading, supplied by Hopkinson pressure bar, drop weight test has used a far-field peak load to calculate the fracture toughness that is locally at the crack tip. In the modified drop weight test, the dynamic fracture toughness can be calculated using the following equation [26]:

$$K_{Ic}^d(t) = 0.25 \times (S/D) \times (P(t)/D^{1.5}) \times Y_I' \quad (2)$$

$$Y_I' = \frac{2 \times (\frac{D}{S}) \times [450.8531 \times (\frac{S}{3.33D})^2 \times (\frac{a}{D})^{1.5}]^{0.5}}{[(\frac{a}{D}) - (\frac{a}{D})^{2}]^{0.25}} \quad (3)$$

where S is the support span (m), a is the crack length (m), D is the diameter of the core (m), P is the applied load (N), and Y_I' is the dimensionless stress intensity factor.

Having the dynamic fracture toughness and the elastic modulus (E), the fracture energy (G) can be calculated using the following equation [27].

$$G = \frac{(K_{Ic}^d)^2}{E} \quad (4)$$

The dynamic experimental results are listed in Table 4.

Table 4. Results of experimental tests.

Test No.	Height of falling weight (m)	Loading rate (kN/μS)	Maximum load (kN)	Dynamic fracture toughness (MPa√m)	Fracture energy ($\frac{J}{m^2}$)
C1	0.3	0.12	16.7	9.6	1249.73
C2	0.6	0.28	21	12.14	1998.54
C3	0.3	0.15	17.5	10.12	1388.78
C4	0.6	0.29	22	12.73	2197.51
C5	0.9	0.36	26.5	15.33	3186.83
C6	1.2	0.56	32	18.51	4646.08
C7	0.3	0.17	18.6	10.76	1570
C8	0.9	0.37	25.5	14.75	2950.25
C9	1.2	0.52	31	17.93	4359.48

The measured dynamic fracture toughness and dynamic fracture energy at different loading rates are plotted in Figure 9. The results obtained indicate that the dynamic fracture toughness of the limestone core specimen for loading rates from 0.12 to 0.56kN/μS was between 9.6 and 18.51 MPa.√m, which is linearly growing with increase in the loading rate. The range of dynamic fracture energy is from 1249.73 to 4646.08 $\frac{J}{m^2}$, in a linear form when the loading rate increases.

5. Numerical simulations

The numerical simulations corresponding to the experimental tests were done by means of the ABAQUS software. For this purpose, a model of the core specimen was defined in the software and

a crack was introduced to the model, as illustrated in Figure 10.

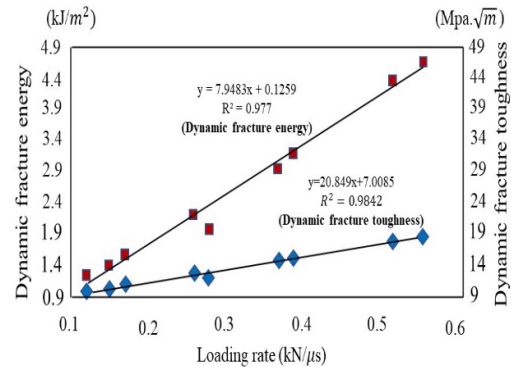


Figure 9. Dynamic fracture toughness and dynamic fracture energy versus loading rate.

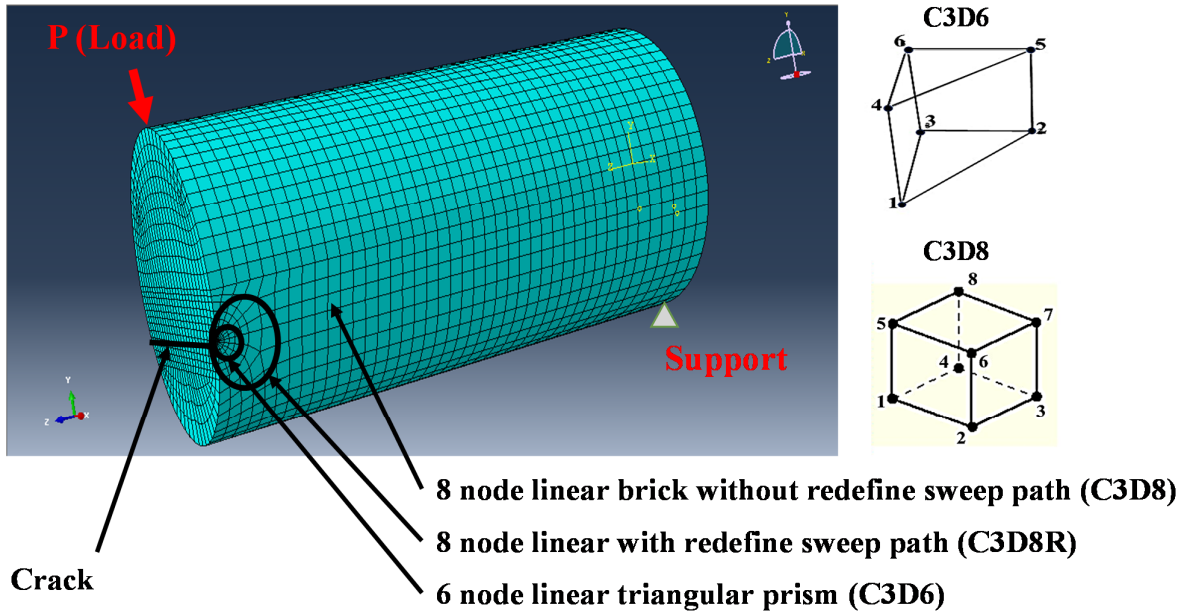


Figure 10. 3D numerical model of core specimen

To calculate the dynamic fracture parameters by J-integral, the far field stress caused dynamic force that has been measured during the experiment is necessary to be linked to the near field stress around the crack tip. In addition, each element has a feature providing flexibility for modelling of different geometry and structure including number of nodes, degree of freedom, and so on. An element's number of nodes determines how the nodal degrees of freedom will be interpolated over the domain of the element. Near the crack tip, the mesh should be fine, provide an accurate result, and be geometrically versatile. Thus 6-node linear triangular prisms (C3D6) were used with a regular arrangement in the position of crack tip to simulate the crack. According to the concept of J-integral, it is necessary to define several independent paths for estimation of the fracture parameters to avoid Hourglass and locking in simulation. Therefore, an 8-node linear brick with redefined sweep path (C3D8R) was used to create a circular path around the crack tip to calculate the J-integral. Furthermore, to adapt the rest of the numerical model with the used element and reduce the computation time, an 8-node linear brick without redefined sweep path (C3D8) was used to complete the model.

The J-integral method in the ABAQUS software was verified by exact analytical solution of fracture mechanics and proved to be authentic for comparison. In the J-integral method, a number of independence contour integrals are defined around

the tip according to the theorem of energy conservation. The form of these integrals can be written as follows:

$$J = \oint (w dy - t \frac{\partial u}{\partial x} dr) \quad (5)$$

$$w = \int_0^\epsilon \sigma_{ij} d\varepsilon_{ij} \quad (6)$$

where w is the density of the strain energy, Γ is a closed counter-clockwise contour presented in Figure 11, t is the traction vector defined by the outward drawn normal n and t ($t = \sigma n$), σ is the stress tensor, ε is the strain tensor, u is the displacement vector, and $d\Gamma$ is the element of the curve along the path Γ [27].

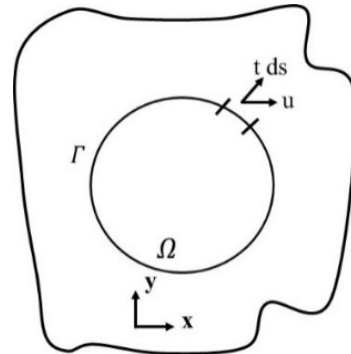


Figure 11. J-Integral definition around a crack [27]

The half-sinusoidal dynamic load recorded during the experimental test was applied to the numerical

model. To correctly simulate the dynamic response of an infinite domain with a finite model, the viscous boundary with a high absorbing capacity is necessary. Therefore, the infinite element (CINPE4) in the software was used in the boundary of the numerical model. This element eliminates the reflected wave in boundary and the true results can be achieved. The Rayleigh damping was specified in the software with a damping ratio of 10%.

By paying attention to the concept of path independence contour integral and the energy changes during the crack growth, the J-integral at the tip of the crack will be equal to the fracture energy ($J = G$). Finally, the output of the numerical model as the dynamic stress intensity factor and the fracture energy calculated by J-integral function was recorded. The results of the numerical calculation are presented in Table 5.

Table 5. Results of the numerical simulation.

Test No.	Loading rate (kN/μS)	Maximum load (kN)	Dynamic fracture toughness ($MPa\sqrt{m}$)	Fracture energy ($\frac{J}{m^2}$)
C1	0.12	16.7	9.45	1210.32
C2	0.28	21	11.91	1924.1
C3	0.15	17.5	9.94	1339.06
C4	0.29	22	12.46	2107.02
C5	0.36	26.5	15.01	3056.31
C6	0.56	32	18.18	4481.47
C7	0.17	18.6	10.56	1512.43
C8	0.37	25.5	14.45	2832
C9	0.52	31	17.62	4207.78

6. Comparison of experimental and numerical results

The values for the dynamic fracture parameters obtained from the experimental tests and the numerical simulations are compared in Table 6 and Figure 12. According to this table, the difference between the numerical and experimental results is less than 4%, which is due to the simplification and restriction applied to the numerical models. Therefore, this comparison presents that the new experimental technique can be an applicable and reliable method for measurement of the dynamic fracture parameters.

Based on the experimental results, the dynamic fracture toughness and dynamic fracture energy increases with the loading rate. This phenomenon can be explained through the energy of dynamic wave and crack propagation velocity. On the other hand, the crack propagation velocity in brittle specimens limits the maximum velocity below the Rayleigh wave speed. Thus the maximum speed of crack propagation in the specimen takes the minimum time for failure. Regarding this, by increasing the loading rate, the dynamic energy exerted to the specimen will be increased.

Table 6. Comparison of the experimental and numerical results.

Test No.	Loading rate (kN/μS)	Dynamic fracture toughness ($MPa\sqrt{m}$)			Fracture energy ($\frac{J}{m^2}$)		Difference (%)
		Experimental	Numerical	Difference (%)	Experimental	Numerical	
C1	0.12	9.6	9.45	1.6	1249.73	1210.32	3.2
C2	0.28	12.14	11.91	1.9	1998.54	1924.1	3.7
C3	0.15	10.12	9.94	1.8	1388.78	1339.06	3.6
C4	0.29	12.73	12.46	2.1	2197.51	2107.02	4.1
C5	0.36	15.33	15.01	2.1	3186.83	3056.31	4
C6	0.56	18.51	18.18	1.8	4646.08	4481.47	3.5
C7	0.17	10.76	10.56	1.9	1570	1512.43	3.7
C8	0.37	14.75	14.45	2	2950.25	2832	4
C9	0.52	17.93	17.62	1.7	4359.48	4207.78	3.5

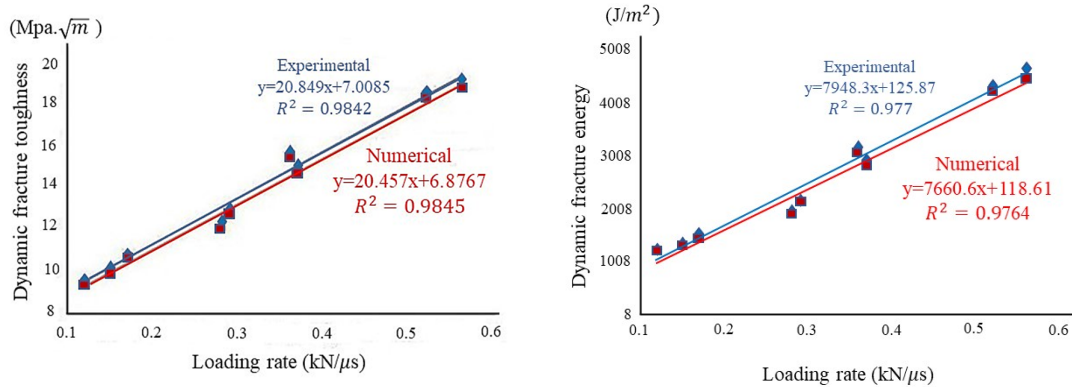


Figure 12. Comparison between the numerical and experimental results.

7. Conclusions

The conventional drop weight test for measurement of dynamic fracture toughness of metals has some limitations in application for rocks. These limitations are due to a sudden impact in the drop weight test, which leads to a jump in the specimen from its supports. It may result in a lack of recording the reflected wave from interface of specimen and the tub head, and therefore, no stress equilibrium during the test. This research work has introduced the development of a new experimental technique in the drop weight test machine to improve the drawbacks of the test. For this purpose, the idea of wave transmission bar was borrowed from the Hopkinson pressure bar test and applied to the drop weight test in order to develop a modified setup for drop weight test machine. By this technique, the specimen will not jump of when the weight is dropped, and consequently, it will easily achieve the stress equilibrium, and the reflected wave from interface of specimen and tub head can be recorded. Furthermore, the rate and form of the compressive loading is not dependent on the features of the specimen and the machine. Another advantage of the modified setup system is that the larger rock specimens that could be tested in a variety of forms including disc-shaped, cylindrical, and cubic. In order to verify the applicability and reliability of the developed technique, the dynamic behavior of some limestone core specimens was studied. The rock samples were tested using the modified machine and all the tests were simulated in the ABAQUS software. The dynamic fracture toughness and dynamic fracture energy of the limestone core specimens under the loading rates of 0.12-0.56kN/μs were measured between 9.6-18.51MPa√m and 1249.73-4646.08J/m², respectively. The comparison of the numerical and experimental results showed a good agreement, where the difference was less than 4%.

Therefore, it can be concluded that the new experimental technique can be used for measurement of the dynamic fracture parameters of rocks. It is noticeable that as this work is limited to a unique type of rock material, limestone, more tests on different rock materials are essential for confirmation of the application of the developed technique for a wider range of rock types.

References

[1]. Khandouzi, G.H., Mollashahi, M. and Moosakhani, M. (2019). Numerical simulation of crack propagation behavior of a semi-cylindrical specimen under dynamic loading. *Frattura ed Integrità Strutturale*. 50:29-37; DOI: 10.3221/IGF-ESIS.50.04.

[2]. Saghafi, H.A., Ayatollahi, M.R. and Sistani, M. (2010). A modified MTS criterion (MMTS) for mixed mode fracture toughness assessment of brittle materials. *Material science and engineering: A*. 527:5624-30.

[3]. Chen, C.S. Pan, E. and Amadei, B. (1998). Fracture mechanics analysis of cracked discs of anisotropic rock using the boundary element method. *International journal of rock mechanics & mining sciences*. 35:195-218.

[4]. Khandouzi, G.H., Mirmohammadlou, A. and Memarian, H. (2014). Dynamic fracture behavior of cubic and core specimen under impact load. *Rock engineering and rock mechanics*. 149-54. DOI: 10.1201/b16955-22.

[5]. Franklin, J.A. and Atkinson, B.K. (1988). Suggested methods for determining the fracture toughness of rock. *Int J Rock Mech Min Sci goe-mechanics Abstract*. 25 (2):71-96.

[6]. Fowell, R.J., Xu, C. and Chen, J.F. (1995). Suggested method for determining mode-I fracture toughness using cracked chevron-notched Brazilian disc (CCNBD) specimens. *Int J Rock Mech Min Sci goe-mechanics Abstract*. 32 (1):57-64.

[7]. Chunan. T. and Xiaohe, X. (1990). A new method for measuring dynamic fracture toughness of rock,

engineering fracture mechanics. International journal of fracture Mechanics. Vol. 35, NO. 4/S, pp. 783-791.

[8]. Wang, Q.Z., Feng, F., Ni, M. and Gou, X.P. (2011). Measurement of mode I and mode II rock dynamic fracture toughness with cracked straight through flattened Brazilian disc impacted by split Hopkinson pressure bar. Engineering Fracture Mechanics. 78:2455–69.

[9]. Wang, Q.Z., Zhang, S. and Xie, H.P. (2009). Rock Dynamic Fracture Toughness Tested with Holed-cracked Flattened Brazilian Discs. Proceedings of the International Congress and Exposition, Orlando, Florida USA. 50:877-85.

[10]. Nikita, F. Morozov., Yuri, V. petrov., Vladimir, I. Smirnov. (2009). Dynamic Fracture of Rocks. 7th EUROMECH Solid Mechanics Conference. Lisbon, Portugal. September 7th-11th.

[11]. Chen, R. Xia, K., Dai, F., Lu, F. and Luo, S.N. (2009). Determination of dynamic fracture parameters using a semi-circular bend technique in split Hopkinson pressure bar testing. Engineering Fracture Mechanics. 76:1268–76.

[12]. Dai, F., Chen, R., Iqbal, M.J. and Xia, K. (2010). Dynamic cracked chevron notched Brazilian disc method for measuring rock fracture parameters. International Journal of Rock Mechanics & Mining Sciences. 47: 606–13.

[13]. Yao, W. and Xia, K. (2019). Dynamic notched semi-circle bend (NSCB) method for measuring fracture properties of rocks: Fundamentals and applications. Journal of rock mechanics and geotechnical engineering. 11: 1066-1093.

[14]. Shi, X., Yao, W., Liu, D., Xia, K., Tang, T. and Shi, Y. (2019). Experimental study of the dynamic fracture toughness of anisotropic black shale using notched semi-circular bend specimens. Engineering fracture mechanics. 205: 136-151.

[15]. Liu, X.R., Yang, S.Q., Huang, Y.H. and Chen, J.L. (2019). Experimental study on the strength and fracture mechanism of sandstone containing elliptical holes and fissures under uniaxial compression. Engineering fracture mechanics. 205: 205-217.

[16]. Omer, Y.B., ozkan, o. and Atban, R.A. (2017). The effect of nanosilica on charpy impact behavior of

glass/epoxy fibr rienfoced composite laminate. Periodical of engineering and natural science, 5: 322-327.

[17]. Abrate, S. (2011). Impact engineering of composite structures. Springer Wien New York, Printed in Italy. ISBN 978-3-7091-0522-1.

[18]. Lorriot, T., Martin, E., Quenisset, J.M. and Rebiere, J.P. (1998). Dynamic analysis of instrumented CHARPY impact tests using specimen deflection measurement and mass-spring models. International Journal of Fracture. (91):299-309.

[19]. Jiang, F. and Vecchio, K.S. (2009). Hopkinson Bar Loaded Fracture Experimental Technique: A Critical Review of Dynamic Fracture Toughness Tests. Applied Mechanics. DOI: 10.1115/1.3124647.

[20]. Chunhuan, G., Fengchun, J., Ruitang, L. and Yang Y. (2011). Size effect on the contact state between fracture specimen and supports in Hopkinson bar loaded fracture test. Int JFract.169:77–84.

[21]. Sheikh, A. K., Arif, A.F.M. and Qamar, S.Z. (2002). Determination of fracture toughness of tool steels. The 6th Saudi Engineering Conference, KFUPM, Dhahran. 5:169.

[22]. Zhang, B.Q. and Zhao, J. (2014). A review of dynamic experimental techniques and mechanical behavior of rock materials. Rock mechanic and rock engineering. (47):1411-78.

[23]. Manhan, M.P. and Stonesifer, R.B. (2007). Studied toward optimum instrumented striker designs. European structure integrity society. (30):221-8.

[24]. Knapp, J., Altmann, E., Niemann, J. and Warner, K.D. (1998). Measurement of shock events by means of strain gauges and accelerometers. Measurement Elsevier. (24):87-96.

[25]. Lou, J., Ying, K., He, P. and Bai, J. (2005). Properties of Savitzky–Golay digital differentiators. Digital Signal Processing. (18):122-36.

[26]. Ouchterlony, F. (1981). Extension of compliance and stress intensity formulas for the single edge cracked round bar in bending. ASTM STP 678. 166-182.

[27]. Saouma, V.E. (2000). Lecture Notes in fracture mechanics. CVEN.6831, University of Colorado, Boulder. CO:80309-0428, 2000.

ارائه یک روش جدید آزمایشگاهی برای اندازه‌گیری چقرمگی شکست دینامیکی سنگ‌ها با استفاده از آزمون سقوط وزنه

قربان خاندوزی¹، حسین معماریان¹ و محمدحسین خسروی^{*1}

دانشکده مهندسی معدن، پردیس دانشکده‌های فنی دانشگاه تهران

ارسال 2020/06/20، پذیرش 2020/07/09

* نویسنده مسئول مکاتبات: mh.khosravi@ut.ac.ir

چکیده:

خصوصیات شکست دینامیکی نمونه‌های سنگی نقش مهمی در تحلیل موضوعات شکست از قبیل انفجار، شکست هیدرولیکی و طراحی نگهدارنده‌ها ایفا می‌کند. چندنین روش آزمایشگاهی برای اندازه‌گیری خصوصیات شکست دینامیکی نمونه‌های سنگی توسعه یافته است. با این وجود، بسیاری از دستگاه‌های آزمایشگاهی برای نمونه‌های فلزی ساخته شده و برای نمونه‌های سنگی مناسب و کارآمد نیست. در این مقاله، روش جدیدی برای اندازه‌گیری چقرمگی شکست دینامیکی و انرژی شکست نمونه سنگی با آزمون سقوط وزنه اصلاح شده توسعه یافته است. ایده میله انتقال دهنده موج از آزمون هاپکینسون گرفته شده و در اصلاح آزمون سقوط وزنه بکار برده شده است. یک نمونه سنگ آهک با دستگاه اصلاح شده سقوط وزنه تست شده و نتایج بدست آمده تحلیل شده است. نتایج نشان داد که چقرمگی شکست دینامیکی و انرژی شکست دینامیکی با نرخ بارگذاری یک رابطه خطی دارند. چقرمگی شکست دینامیکی و انرژی شکست دینامیکی نمونه سنگ آهک در نرخ‌های بارگذاری 0/12 تا 0/56 کیلو نیوتن بر میکروثانیه به ترتیب بین مقادیر 9/6 تا 18/51 مگاپاسکال در رادیکال متر و 1249/73 تا 4646/08 ژول بر مترمربع اندازه‌گیری شده است. نهایتاً جهت اعتبارسنجی نتایج دستگاه اصلاح شده سقوط وزنه، یک سری شبیه‌سازی عددی در محیط نرم افزار آباکوس انجام شده است. مقایسه نتایج انطباق خوبی را بین مقادیر بدست آمده آزمایشگاهی و مدلسازی عددی نشان می‌دهد، بطوریکه اختلاف بین نتایج آزمایشگاهی و عددی کمتر از 4 درصد است. بنابراین می‌توان نتیجه‌گیری کرد که تکنیک جدید در اصلاح آزمون سقوط وزنه می‌تواند در اندازه‌گیری بهتر رفتار دینامیکی نمونه‌های سنگی در آزمایشگاه کاربردی باشد. با این وجود، جهت تأیید کارایی تکنیک توسعه یافته در دامنه وسیع‌تری از سنگ‌ها، نیاز به انجام آزمون‌های بیشتر بر روی نمونه‌های متنوع سنگ خواهد بود.

کلمات کلیدی: چقرمگی شکست دینامیکی، تست سقوط وزنه، شبیه‌سازی عددی، سنگ آهک.